Isolative Green Synthesis and Characterization of Cellulose and Cellulose Nanocrystals from *Typha Augostifolia*

Lynda S. Mesoppirr , Evans K. Suter , Wesley N. Omwoyo * , Nathan M. Oyaro , Simphiwe M. Nelana

Posted Date: 14 February 2024

doi: 10.20944/preprints202402.0763.v1

Keywords: *Typha augostifolia*; cellulose; acid hydrolysis; chemically purified cellulose; cellulose nanocrystals

Research Article

Isolative Green Synthesis and Characterization of Cellulose and Cellulose Nanocrystals from *Typha augostifolia*

Lynda S. Mesoppirr [1], Evans K. Suter [1,2], Wesley N. Omwoyo [1,2,*], Nathan M. Oyaro [1] and Simphiwe M. Nelana [2]

[1] Department of Mathematics and Physical Science, Maasai Mara University, Narok-Kenya
[2] Biotechnology and Chemistry Department, Vaal University of Technology, Vanderbijlpark, South Africa
* Correspondence: wesleyomwoyo@mmarau.ac.ke; Tel.: +254-722297602

Abstract: The application potential of cellulosic materials in natural composites and other fields needs to be explored to develop innovative, sustainable, lightweight, functional biomass materials that are also environmentally friendly. This study investigated *Typha augostifolia* (Typha sp.) as a potential new raw material for extracting cellulose nanocrystals (CNCs) for application in wastewater treatment composites. Alkaline treatments and bleaching were used to remove cellulose from the stem fibers. The CNCs were then isolated from the recovered cellulose using acid hydrolysis. The study showed a few distinct functional groups (O-H, -C-H, =C-H and C-O, and C-O-C) in the Fourier Transform Infrared (FTIR) spectra. Scanning electron microscope (SEM) revealed the smooth surface of CPC and CNCs that resulted from removing lignin and hemicellulose from powdered *Typha augostifolia*. Based on the crystalline index, the powdered *Typha augostifolia*, CPC, and CNCs were 42.86%, 66.94% and 77.41%. The loss of the amorphous section of the Typha sp. fiber resulted in a decrease in particle size. It may be inferred from the features of a Typha sp. CNC that CNCs may be employed as reinforcement in composites for wastewater treatment.

Keywords: *Typha augostifolia*; cellulose; acid hydrolysis; chemically purified cellulose; cellulose nanocrystals

1. Introduction

Cellulose is a widely available, fiber-forming polymer made from universal units. The units of β-1,4-linked glucopyranose found in cellulose form a naturally occurring linear homopolymer with a high molecular weight [1]. Cellulose consists of three hydroxyl groups that are present in each glucopyranose molecule, giving it properties like biodegradability, biocompatibility and insolubility in water. It also serves as the protective wall for plant cells. The degree of polymerization in cellulose obtained from wood can reach 10,000 units, but that derived from cotton has 15,000 units [2,3]. Plant cell walls, such as those found in giant reed, sugarcane bagasse, cotton stalk waste, date seeds, roselle fibers, mengkuang (*Pandanus artocapus*) leaves, waste cotton textiles, and *Typha domingensis* plants, are the primary source of cellulose [3–10]. Other small sources of cellulose include marine creatures (tunicates), algae, bacteria, fungus, and anchovies [11].

Typha is a member of the 30 species-strong Typhaceae family. The genus is known in American English as cattail but in British English as reedmace or bulrush [4]. Wetlands are ideal habitats for the herbaceous grass *Typhaceae augostifolia*. According to Yamauchi et al. (2013), the plant is perennial and has rhizomes with a well-developed aerenchyma system, enabling survival in its particular wetland ecosystem [12]. Among the Typha sp. *Typha angustifolia* L. can survive in highly salinized environments, grows in the estuary, meadow grass, fen, and marsh.

 doi:10.20944/preprints202402.0763.v1

Actually, T. angustifolia L. serves as a macrophyte that may remove harmful metals and toxins by immobilizing them in the sediment and reintroducing them into the earth's geological cycle [12]. In addition, *Typha angustifolia* L. can emit exudates, promote phytovolatilization, carry oxygen into the rhizosphere, and provide donor surfaces that are absorbent and conducive to biofilm formation [13]. Through phytoremediation, *Typha angustifolia* L can eliminate dichloroethane up to 100% for 42 days [14]. Moreover, it may be used as a source of cellulose and to remove methylene blue dye [15,16]. The plant's high biomass accumulation in its tissues and excellent resilience to stress make it a popular choice for treating wastewater in wetland environments [17]. However, T. angustifolia L. has not fully exploited extensively, people frequently overlook and disregard its presence.

Cellulose consists of amorphous and crystalline phases, these phases are joined together by hydrogen bonds that are both intra- and intermolecular. As a result, heat does not readily break down cellulose [18]. Five distinct polymorphs of cellulose biopolymers are known to exist. Cellulose I to V are examples of cellulose polymorphs. Natural cellulose found in crystallized form is called cellulose I. Subsequently, it can undergo further chemical processing, such as precipitation from the solution or the maceration process (treatment with strong sodium hydroxide solution) to transform it into cellulose II [19].

According to Kumar et al. (2010), nanotechnology has become a rapidly expanding multidisciplinary topic of study in the creation of cellulose-based nanocrystals (CNC), cellulose nano whiskers (CNW), and cellulose nanoparticles (CNP) from easily grown annual plants or agricultural wastes that are readily available locally. Enzymatic hydrolysis, carbon catalyst, and high-pressure homogenization are a few techniques that may be used to isolate cellulose nanocrystals. Using acids or bases as the solvent in a hydrothermal reactor for hydrolysis also serves as a catalyst for the breakdown of the molecules into smaller pieces [20]. The amorphous phase of the cellulose may be easily removed by hydrolysis with an acid. The degree of polymerization decreased as a result, producing thicker and shorter crystals [21]. The process involves the assault of loose, amorphous portions of cellulose by hydrogen ions from acids, which breaks the 1,4-glycoside linkages, leaving the crystalline sections of cellulose intact [22]. Following chloride acid hydrolysis, cellulose has a thermal strength of 363.9 °C, more significant than that of sulfate and phosphate acids. It also exhibits a yield of 93.7% and a crystallinity of about 88.6% [23]. In some studies, Date palm seeds were processed into microcrystalline cellulose by Abu-Thabit et al. using HCl 2.5 N (1:11 w/v), and a temperature of 85 °C produced a crystalline index of 70% [24].

Acid hydrolysis is often conducted with the use of ultrasonic method. This method employs a lower temperature for organic compounds, which may boost yield and shorten reaction times, and it has high selectivity. After lignin and hemicellulose are extracted from lignocellulose, the ultrasonic approach helps dissolve the biomass during the separation process of microcrystalline or nanocrystalline cellulose. This method results in a cellulose solution with smaller particle sizes (<0.5 mm), a stable colloid, and easy enzyme accessibility [25].

In this work, our aim was to prepare chemically purified cellulose (CPC) from *Typhacea augostifolia* by the process of dewaxing and delignification using 10% nitic acid and 1M sodium hydroxide and bleaching using Sodium hypochlorite. The prepared CPC were acid hydolzed using 32% H_2SO_4 to obtain cellulose nanocrystals.

2. Materials and Methods

2.1. Materials

Typha augostifolia grass was harvested from Maasai Mara University botanical garden, Narok Kenya (1° 41′ 5.2872″ N and 37° 20′ 27.096″ E), altitude of 1827 M above sea level. The grass of about 4 meters tall was harvested by cutting, chopped into smaller pieces, washed with distilled water and air dried in the laboratory (Figure 1). It was then ground into fine powder and packed in sealed plastic bags ready for dewaxing and delignification.

 doi:10.20944/preprints202402.0763.v1

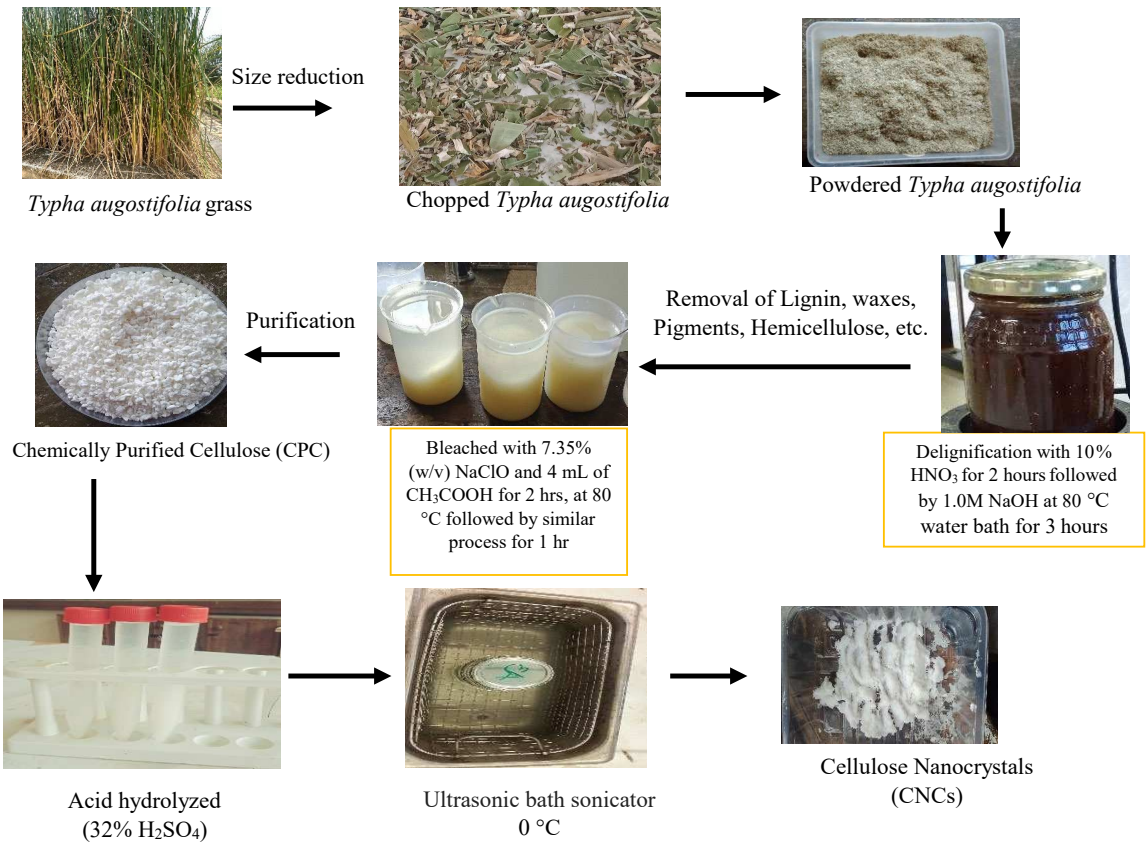

Figure 1. Summarized schematic diagram for synthesizing CNCs.

Other chemicals and reagents employed in the study were analytical grade, sodium hydroxide (NaOH ≥ 98%), sulfuric acid (H_2SO_4, >98%), distilled water, sodium hypochlorite (NaOCl, ≥ 75%), acetic acid (≥ 99%), and acetone (≥ 99.9%). The chemicals were purchased from Sigma-Aldrich and were used without further purification.

2.2. Methods

2.2.1. Dewaxing and Delignification

The procedure is summarized in (Figure 1). The dewaxing and delignification process was performed by soaking 50 g of the dried *Typha augostifolia* grass powder in 10% nitric acid at 80 °C for 2 hours, then washed. It was then followed by alkaline pre-treatment where 50 g of *Typha augostifolia* powder was mixed with 500 mL of 1.0M NaOH in a reactor at temperature 80 °C in a hot water bath and maintained at the same temperature under vigorous stirring at 800 rpm for 3 hours. The formed cellulose fibers were quenched with cold deionized water and then washed until neutral. It was then stored for purification.

2.2.2. Chemical Purification (Bleaching)

The obtained cellulose fibers were refluxed with 350 mL (7.35% (w/v)) sodium hypochlorite followed by 4 mL acetic acid (Figure 1). The reaction mixture was agitated for 2 hours at 80 °C with constant stirring at 500 rpm. The residue (Chemically purified cellulose) was then filtered using a Büchner funnel connected to a vacuum pump and rinsed with deionized water until it reached a neutral pH. Before acid hydrolysis, it was treated with acetone for 30 minutes in a Soxhlet chamber to remove impurities like wax, fat, etc. It was then dried at room temperature for three days.

 doi:10.20944/preprints202402.0763.v1

2.2.3. Synthesis of Nanocellulose

Figure 1 illustrates a scematic process. In a 500 mL conical flask, 20 g of chemically purified cellulose (CPC) was combined with 400 mL (32% w/v) sulfuric acid. The synthesis process involved, using a 1:20 (g: mL) cellulose to acid ratio, the mixture was heated in a water bath for 45 minutes. The solution was first heated to 45 °C, then to 55 °C with constant stirring at 600 rpm. The hydrolysis process was stopped by carefully quenching it with 200 mL of 10-fold deionized water five times. The resultant suspension was homogenized using a centrifuge for 40 minutes at 10000 rpm. This process was repeated five times, each time removing the supernatant from the sediment and replacing it with new distilled water until the supernatant's pH was neutral. After three days of room temperature drying, the resulting CNCs were packaged for characterization.

2.3. Characterization

2.3.1. Fourier Transform Infrared (FTIR) Analysis

The functional groups in the *Typha augostifolia* grass powder, chemically purified cellulose, and the nanocellulose were determined using Thermo Scientific Nicolet iS10 (Smart iTR) FTIR spectrometer with a diamond-based ATR compartment. The spectral resolution was set to 4 cm^{-1} over a 4000 and 500 cm-1 wavelength range. For each spectrum, an average of 16 scans were captured, and the primary absorption peaks were identified.

2.3.2. X-Ray Diffraction (XRD) Analysis

The XRD pattern and degree of crystallinity of *Typha augostifolia* grass powder, CPC, and CNCs was assessed using Siemens D5000 X-ray diffractometer at room temperature. A monochrome step scanner Cu-K radiation set at a wavelength of 0.1538 nm was used to scan the samples with a 2θ from 10° to 80° scan angles, and 0.02 and 5.0 min scanning times. The crystallinity index (CrI) was calculated using Equation (1) below.

$$C_rI\ (\%) = \frac{I_{002} - I_{am}}{I_{002}}\ x\ 100 \quad (1)$$

where I_{002} and I_{am} represent the intensity of the peak of crystalline and amorphous regions. Meanwhile, the Scherrer equation (Equation (2)) was used for the crystal methods' size empirically.

$$Cystal\ size\ (D) = \frac{K\lambda}{\beta \cos\theta} \quad (2)$$

From the equation the crystal structure has a K factor of 0.89, λ is the length of a light wave (1.54056 Å), β is the Full Width at Half Maximum (FWHM) in radians, and θ is the angle of diffraction in degrees.

2.3.3. Scanning Electron Microscope-Electron Dispersive Spectroscopy (SEM-EDS) Analysis

Surface morphology of *Typha augostifolia* grass powder, CPC, and CNCs was examined using a scanning electron microscope (JEOL-IT 7500LA, Japan) with an accelerating voltage of 15-20 kV. The samples were sputtered with a thin coating of gold metal after being placed on a carbon tape metal stub. While for elemental analysis, electron dispersive spectroscopy (EDS) (JSM-IT500, JEOL Ltd., Tokyo, Japan) was used to determine the percentage purity of the samples.

2.3.4. Thermogravimetric (TGA) Analysis

TGA was used to quantify the loss of mass for the *Typha augostifolia* grass powder, CPC, and CNCs under a controlled temperature change in a nitrogen atmosphere. Approximately 18.00 mg samples were examined using Mettler Toledo Thermogravimetric analyzer linked to an inert nitrogen gas flow and pyrolyzed at a rate of 10 °C/min from 30 °C to 1000 °C.

 doi:10.20944/preprints202402.0763.v1

3. Results

3.1. Physical Appearance

Figure 2a–d depicts the physical characteristics of the raw chopped *Typha augostifolia* as collected from the field without any chemical treatments, the powdered *Typha augostifolia*, the chemically purified cellulose before and after acid hydrolysis. The chemical alteration caused the *Typha augostifolia* to become whiter in colour. Both the raw and powdered *Typha augostifolia* were green and brown, as seen in Figure 2a,b. The cellulose (white powder) was formed by treating *Typha augostifolia* powder with HNO_3, NaOH, and sodium hypochlorite (Figure 1c). Whiter and gel, hairy-like material (cellulose nanocrystals) was obtained by hydrolyzing the recovered cellulose with H_2SO_4 acid and then washing with acetone (Figure 2d). Similar results were obtained by Evans et al. (2019), who isolated cellulose from sugar cane bagasse then synthesized cellulose nanocrystals from it though acid hydrolysis [9]. This established that chemical treatment with NaOH, and purification (bleaching with (NaClO) makes the fiber to change color. In a different research, Johar et al. (2012) treated rice husk fibers at various stages and observed and described their physical and chemical characteristics. When the rice husk was treated with an alkaline solution, it lost its brown color and became entirely white [26]. The observed changes were all associated with the elimination of wax, pigments like chlorophyll, lignin, hemicellulose, etc.[27]

Figure 2. Physical appearance of (a) Chopped *Typha augostifolia* green leaf (b) Dried and crushed *Typha augostifolia*, (c) Isolated cellulose from *Typha augostifolia* and (d) Cellulose nanocrystals from *Typha augostifolia.*

3.2. Functional Group Analysis (FTIR)

The functional groups for the *Typha augostifolia*, chemically purified cellulose and cellulose nanocrystals is illustrated in Figure 3. The major absorption bands corresponding to different groups for the grass material all the way to the nanocellulose were observed as from 500 cm^{-1} to around 3600 cm^{-1}. The broad peak at around 3309 cm^{-1} is linked to intramolecular hydrogen bond O-H stretching, which was seen in all the materials. Similarly, all materials exhibit the C-H stretching of the cellulosic materials, with only minor shifts and variations in intensity, at the peaks around 2892 and 2915 cm^{-1}. The wavenumber around 898 cm^{-1} is attributed to the C-H rocking vibration of cellulose in all materials. The bands at 1034 cm^{-1}, 1730 cm^{-1} and 1632 cm^{-1} are due to C-O-C of the pyranose ring, carboxyl groups found in esters and acids that are primarily found in lignin and O-H bending vibrations respectively. The peak at 1730 cm^{-1} was only observed in the *Typha augostifolia* grass powder and is due to the esters and acids only present in the lignin. The peak was not seen in CPC, and CNCs samples, a clear indication that the esters and acids were successfully removed. At around 1157 cm^{-1}, a peak of O-H associated with C-O-H was present and was bigger and well-defined in cellulose than the rest of the samples, indicating a purer sample. The O-H peak associated with absorbed water at around 1632 cm^{-1} was constant for all the samples.

 doi:10.20944/preprints202402.0763.v1

The major difference between the grass sample and the cellulosic materials was noted at around 1245 cm^{-1}, this peak is attributed to C=C of aromatic rings, an indication of a mixture of other organic compounds, aromatic in nature, found in plants' matrix like phenols and lignin. The peak was not present in the delignified grass and the chemically purified cellulose, indicating that lignin and all the other compounds were completely removed.

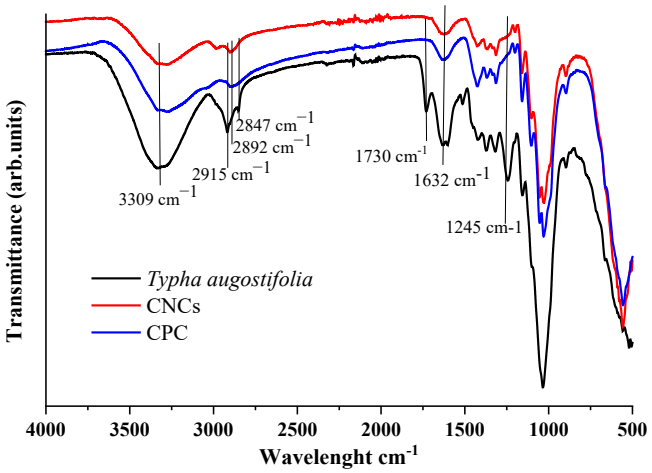

Figure 3. FTIR spectra of *Typha augostifolia*, CPC, and CNCs.

3.3. Scanning Electron Microscopy (SEM)

Using scanning electron microscopy, the shape and diameter of the CPC and CNCs were determined and presented Figure 4a–c. From the SEM images, the *Typha augostifolia* display regular rod-like structures that are not chemically connected with spongy-like and loose materials stuck on its rough surface indicating that the materials are of different composition (Figure 4a). On dewaxing and delignification, it is seen that the CPC structures are not fused despite having a lengthy, uneven form (Figure 4b). The smooth surface of the cellulose results from lignin and hemicellulose being extracted from powdered *Typha augostifolia* [28]. The amorphous and crystalline portions of microcrystalline cellulose are still fused together, resembling a continuous thread. The cellulose had the same form as the other references [13,19,29]. Meanwhile, after H_2SO_4 hydrolysis, CNCs (Figure 4c) demonstrate that only crystalline regions remain since H_2SO_4 breaks down the amorphous regions. The size of the powdered Typha augostifolia, the chemically purified cellulose was 271.67±3.02 µm, 161.15±3.83 µm, and 98.57±2.54 nm before and after hydrolysis.

 doi:10.20944/preprints202402.0763.v1

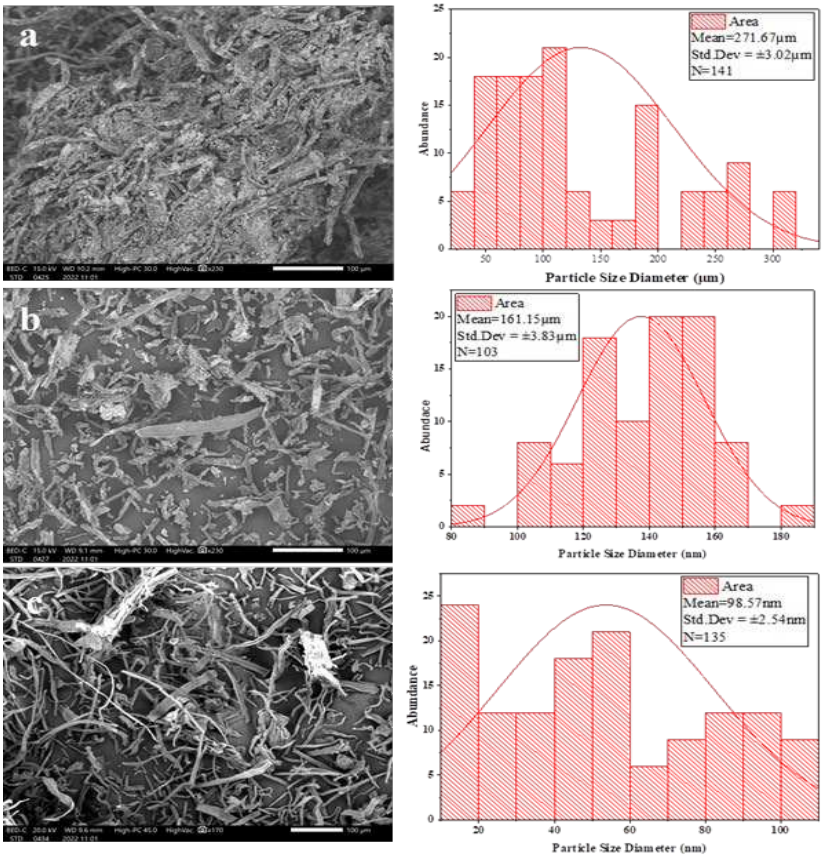

Figure 4. Scanning electron (SEM) images (a) *Typha augostifolia*, (b) CPC, and (c) CNCs.

3.4. Elemental Analysis

The quantification of the composition of elements present in the *Typha augostifolia*, the prepared cellulosic materials done using Electron Diffraction Spectroscopy (EDS) is shown in Figure 5a–c. The analysis was performed to further investigate the composition of the isolated cellulose and the synthesized CNCs (Figure 5b,c). From the *Typha augostifolia* EDS spectrum, C and O, the main building blocks of cellulose, were quantified to be 51.60±0.13%, and 48.35±0.27%. While traces of Ca and Fe were found to be 0.04±0.01%, and 0.01±0.01%, respectively. The trace elements could be attributed to nutrients initially present in the *Typha augostifolia* grass. However, for the cellulosic materials carbon and oxygen atoms constituted 52.29±0.23% and 47.71±0.46% for CPC and 59.75±0.18% and 40.25±0.35% for CNCs. The elemental analysis showed the purity of the cellulose formed which is made purely of carbons and oxygen. On H_2SO_4 hydrolysis, it noted that there is an increase in C percentage with decrease in that of O. Studies indicate that the breakdown of cellulose into smaller components (cellulose nanocrystals) results in the removal of oxygen-containing functional groups [30]. This further confirmed that the isolation of cellulose and synthesis of its nanocrystals was successfully achieved.

 doi:10.20944/preprints202402.0763.v1

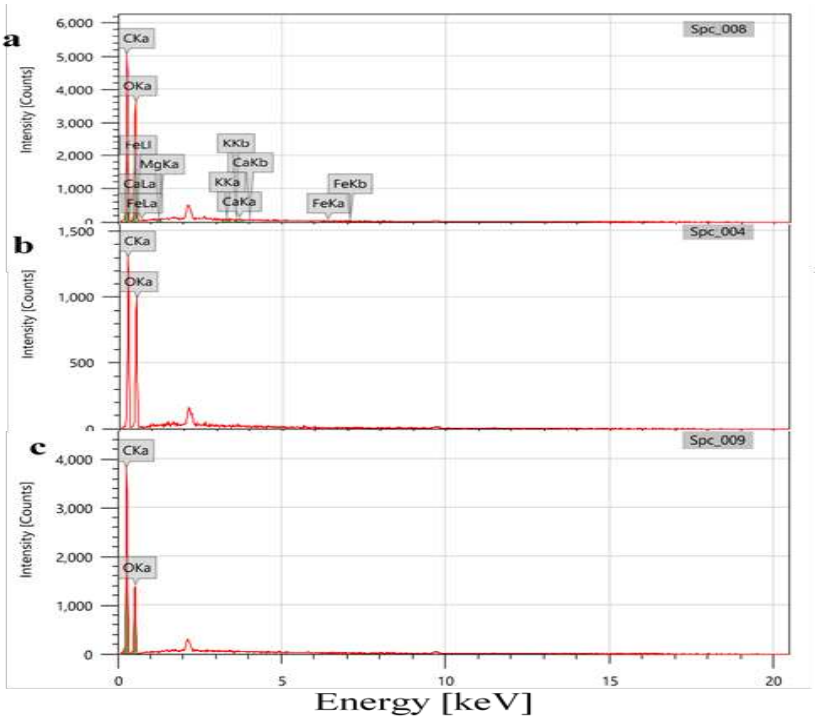

Figure 5. EDS spectrum of *Typha augostifolia*, CPC, and CNCs.

3.5. Crystalline Structure Analysis X-ray Diffraction

Figure 6 shows the crystal structures while Table 1 shows the crystallinity indices of *Typha augostifolia* powder, CPC and CNCs. While the peaks in each sample varied in intensity, they all displayed similar patterns except for *Typha augostifolia* grass powder. Cellulose polymorphs I and II correspond to either CNCs or CPC. High amounts of NaOH added to *Typha augostifolia* grass powder changed the cellulose properties from cellulose I to cellulose II. The (101) crystalline planes of hemicellulose are thought to be responsible for the first XRD peak [31]. The (002) planes from the monoclinic structure of cellulose I are referred to as the second peak [32,33]. Similarly, the third XRD reflex, which appears as a blurred band, confirms the presence of the (040) crystal faces from the amorphous areas (primarily lignin and hemicellulose).It is reported that for cellulose I and cellulose II, the peak intensity values of crystal cellulose are 2θ = 22.5° and 2θ = 20.1°, respectively. The highest intensity value of amorphous cellulose is 2θ = 18° for cellulose I and 2θ = 16.3° for cellulose II [28]. From Figure 4a the cellulose's post-hydrolysis peak pattern shows that crystalline cellulose I have a typical structure on the peak of 2θ at 22.64°. In contrast, amorphous cellulose II has a typical structure on the peak of 2θ at 15.83°. Crystalline cellulose II, and crystalline cellulose I showed peaks at intensity values of 2θ of 16.23° and 22.58°, respectively, prior to hydrolysis of cellulose. The powdered *Typha augostifolia* showed peaks with intensity values of 2θ of 16.11°, 21.00°, and 22.89° representing amorphous cellulose I, amorphous cellulose II, and crystalline cellulose II [28,34].

Table 1. Crystallinity indices of *Typha augostifolia* grass powder, CPC, and CNCs.

	$2\theta_{(Amorphous)}$ (°)		$2\theta_{(002)}$ (°)		Crystallinity Index
Sample	**Degree**	**Intensity, I_{am}**	**Degree**	**Intensity, I_{002}**	**(*CrI* %)**
Typha augostifolia	21.00	376	34.97	658	42.86
CPC	22.58	287	34.73	868	66.94
CNCs	22.64	211	34.84	934	77.41

Following hydrolysis, the crystallinity of CNCs is better than that of CPC and *Typha augostifolia*. It is evident from each sample's peak intensity. Additionally, it is evident from the peak heights of each sample, upon hydrolysis, cellulose has a greater peak than the others do. Based on the

 doi:10.20944/preprints202402.0763.v1

crystalline index and the size of the powdered *Typha augostifolia*, the cellulose microcrystalline was 42.86% and 308.3 µm, 66.94% and 280.9 µm, and 77.41% and 87.3 nm before and after hydrolysis.

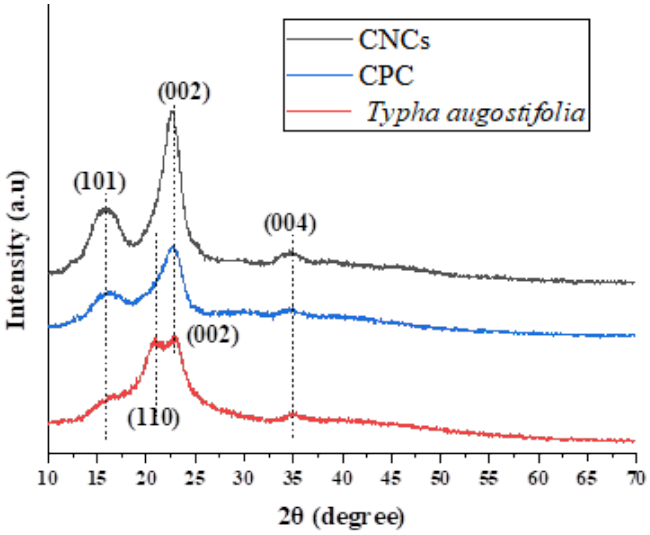

Figure 6. XRD pattern of *Typha augostifolia*, CPC, and CNCs.

3.6. Thermal Analysis

Figure 7a,b with Table 2 provides TGA/DTG data from the thermal degradation mechanisms of powdered *Typha augostifolia*, CPC, and CNCs. The breakdown of hemicellulose happens between 200–260 °C, lignin at 280–500 °C, and cellulose at 340–350 °C, according to Adewale et al. (2022)[35]. The TGA and DTG curves for the samples shown in Figure 7a,b display two main peaks for CPC and CNCs, while *Typha augostifolia* displays three. For all three samples, the emission of water, volatile chemicals, polysaccharides, and other low molecular weight molecules peaked between 70 and 150 °C [9,28]. For CPC, CNCs, and *Typha augostifolia* powder, the percentage weight loss from the first peak in that temperature range was 8.31%, 8.98%, and 14.23%, respectively. The information demonstrated that *Typha augostifolia* powder still had a greater water content than the other samples. The existence absorption band at a peak of 1630 cm^{-1} from the FTIR data on the water's hydrogen bond supports this. The second peak, which ranges from 250 to 350 °C, indicates the presence of cellulose degradation, which indicates polymer and carboxylate elimination, dehydration, and glycosyl breakdown. The second peak's weight loss data was found to be 68.76% of the CNCs, 44.62% of the CPC, and 35.04% of the powdered *Typha augostifolia*. The final degradation indicates an oxidation process and residue breakdown, which is located between 400 and 1000 °C. The final degradation weight loss for powdered *Typha augostifolia* powder was 14.29%, CPC was 2.16%, and CNCs was 2.68%. *Typha augostifolia* powder has higher heat degradation, as indicated by the TGA and DTG curves. It is reported that the benzene ring of the aromatic polycyclic structure of lignin, hemicellulose, and other noncellulose molecules may contribute to this [36]. Compared to CPC and CNCs, *Typha augostifolia* powder in Table 2 has the lowest thermal stability, even though CNCs take the longest decomposing time. It starts to break down at 229.28 °C. The increased thermal stability resulting from the application of H_2SO_4 in acid hydrolysis treatment can be the cause of this [29].

Table 2. Thermal characteristics of Typha augostifolia grass powder, CPC and CNCs.

Temperature	CPC (°C)	CNCs (°C)	Typha augostifolia (°C)
Tonset	253.24	239.01	229.28
Tendset	339.56	344.45	354.06
Td	315.19	315.18	298.32

Following hydrolysis, there was a greater amount of cellulose residue than previously. This might happen when H_2SO_4 was added during the acid hydrolysis procedure. Breakdown of the

 doi:10.20944/preprints202402.0763.v1

cellulose polymer: β-1,4-glycosidic linkages, followed by the generation of levoglucosan and charcoal, was seen at higher temperatures for Typha augostifolia powder, CPC and CNCs [29].

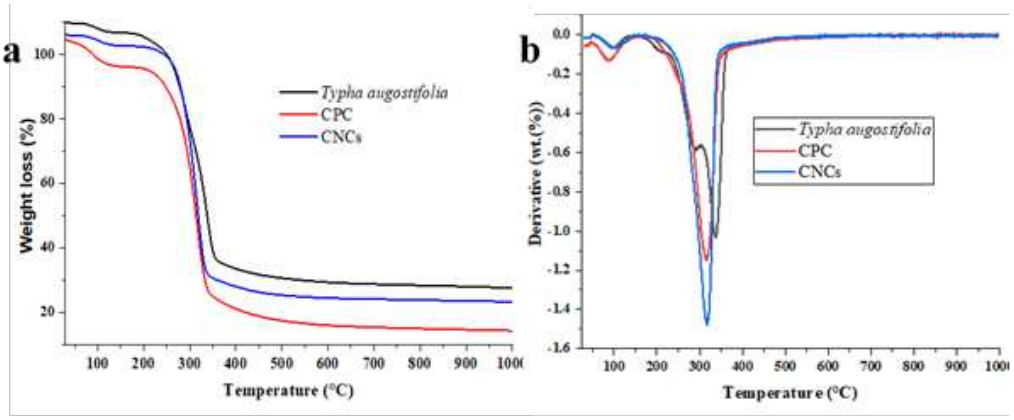

Figure 7. a. TGA and (**b).** DTG curve of *Typha augostifolia*, CPC, and CNCs.

5. Conclusions

The research established that cellulose can be isolated from *Typha augostifolia*. The removal of non-cellulosic materials can be improved through dewaxing and delignification. From the XRD data, the crystallinity of the nanocrystals increased, indicating that the crystalline phase was exposed after the hemicelluloses and lignin, as well as other organic and inorganic components, were successfully eliminated. The particle size was considerably decreased in diameter after acid hydrolysis of cellulose, as revealed by XRD, indicating better CNC characteristics. The findings further indicate that *Typha augostifolia*, a perennial plant with rhizomes with a well-developed aerenchyma system enabling survival in its particular wetland ecosystem, can be employed in extensive production of cellulosic materials.

Author Contributions: Miss. Lynda Mesoppirr collected samples, did formal analysis and investigations and prepared the original draft manuscript. Mr. Evans Suter assisted in sample characterization, methodology and reviewed and edited the draft manuscript. Dr. Wesley Omwoyo provided the conceptualized the study, supervised the work and reviewed and edited the draft manuscript. Prof. N.M. Oyaro was the overal project administrator and also reviwed and edited the draft manuscript. Dr. Simphiwe Nelana coordinated sample characterization in Vaal University of Technology, Northwest University and the University of Witwatersrand all in South Africa, he partly funded the formal analysis part.All the authors have read and agreed to the published version of the manuscript.

Funding: This research received no external funding.

Data Availability Statement: There is no other data other than what is already shared in the manuscript.

Acknowledgments: The authors are thankful to Maasai Mara University for offering laboratory space. The Vaal University of Technology is for FTIR, SEM-EDS analysis, and North West University is for the TGA analysis. The University of Witwatersrand, South Africa, for XRD analysis.

Conflicts of Interest: The authors declare no conflicts of interest.

References

1. Ghanbarzadeh, B.; Almasi, H. Biodegradable Polymers. Biodegradation-life of science 2013, 141–185.
2. Siqueira, G.; Bras, J.; Dufresne, A. Cellulosic Bionanocomposites: A Review of Preparation, Properties and Applications. *Polymers* **2010**, *2*, 728–765.
3. Trache, D.; Hussin, M.H.; Chuin, C.T.H.; Sabar, S.; Fazita, M.N.; Taiwo, O.F.; Hassan, T.M.; Haafiz, M.M. Microcrystalline Cellulose: Isolation, Characterization and Bio-Composites Application—A Review. *International Journal of Biological Macromolecules* **2016**, *93*, 789–804.
4. Pandey, A.; Verma, R.K. Taxonomical and Pharmacological Status of Typha: A Review. *Annals of Plant Sciences* **2018**, *7*, 2101–2106.

5. Barragán, E.U.P.; Guerrero, C.F.C.; Zamudio, A.M.; Cepeda, A.B.M.; Heinze, T.; Koschella, A. Isolation of Cellulose Nanocrystals from Typha Domingensis Named Southern Cattail Using a Batch Reactor. *Fibers and Polymers* **2019**, *20*, 1136–1144.
6. Kian, L.K.; Jawaid, M.; Ariffin, H.; Alothman, O.Y. Isolation and Characterization of Microcrystalline Cellulose from Roselle Fibers. *International Journal of Biological Macromolecules* **2017**, *103*, 931–940.
7. Li, M.; He, B.; Zhao, L. Isolation and Characterization of Microcrystalline Cellulose from Cotton Stalk Waste. *BioResources* **2019**, *14*, 3231–3246.
8. Tlou, S.; Suter, E.; Alfred, M.; Rutto, H.; Omwoyo, W. In Situ Capping of Silver Nanoparticles with Cellulosic Matrices from Wheat Straws in Enhancing Their Antimicrobial Activity: Synthesis and Characterization. *Journal of Environmental Science and Health, Part A* **2023**, *58*, 903–913, doi:10.1080/10934529.2023.2260295.
9. Evans, S.K.; Wesley, O.N.; Nathan, O.; Moloto, M.J. Chemically Purified Cellulose and Its Nanocrystals from Sugarcane Baggase: Isolation and Characterization. *Heliyon* **2019**, *5*.
10. Rani, B.S.J.; Venkatachalam, S. A Neoteric Approach for the Complete Valorization of Typha Angustifolia Leaf Biomass: A Drive towards Environmental Sustainability. *Journal of Environmental Management* **2022**, *318*, 115579.
11. Ismail, M.M.; Elkomy, R.G.; El-Sheekh, M.M. Bioactive Compounds from Components of Marine Ecosystem. *Marine Ecosystems: A Unique Source of Valuable Bioactive Compounds* **2023**, *3*, 206–256.
12. Yamauchi, T.; Shimamura, S.; Nakazono, M.; Mochizuki, T. Aerenchyma Formation in Crop Species: A Review. *Field Crops Research* **2013**, *152*, 8–16.
13. Patro, A.; Dwivedi, S.; Panja, R.; Saket, P.; Gupta, S.; Mittal, Y.; Saeed, T.; Martínez, F.; Yadav, A.K. Constructed Wetlands for Wastewater Management: Basic Design, Abiotic and Biotic Components, and Their Interactive Functions. In *Material-Microbes Interactions*; Elsevier, 2023; pp. 315–348.
14. Al-Baldawi, I.A. Removal of 1, 2-Dichloroethane from Real Industrial Wastewater Using a Sub-Surface Batch System with Typha Angustifolia L. *Ecotoxicology and environmental safety* **2018**, *147*, 260–265.
15. Namasivayam, S.K.R.; Prakash, P.; Babu, V.; Paul, E.J.; Bharani, R.A.; Kumar, J.A.; Kavisri, M.; Moovendhan, M. Aquatic Biomass Cellulose Fabrication into Cellulose Nanocomposite and Its Application in Water Purification. *Journal of Cleaner Production* **2023**, 136386.
16. El Amri, A.; Bensalah, J.; Idrissi, A.; Lamya, K.; Ouass, A.; Bouzakraoui, S.; Zarrouk, A.; Lebkiri, A. Adsorption of a Cationic Dye (Methylene Bleu) by Typha Latifolia: Equilibrium, Kinetic, Thermodynamic and DFT Calculations. *Chemical Data Collections* **2022**, *38*, 100834.
17. Ievinsh, G. Halophytic Clonal Plant Species: Important Functional Aspects for Existence in Heterogeneous Saline Habitats. *Plants* **2023**, *12*, 1728.
18. Wulandari, W.T.; Rochliadi, A.; Arcana, I.M. Nanocellulose Prepared by Acid Hydrolysis of Isolated Cellulose from Sugarcane Bagasse. In Proceedings of the IOP conference series: materials science and engineering; IOP Publishing, 2016; Vol. 107, p. 012045.
19. Trache, D.; Hussin, M.H.; Chuin, C.T.H.; Sabar, S.; Fazita, M.N.; Taiwo, O.F.; Hassan, T.M.; Haafiz, M.M. Microcrystalline Cellulose: Isolation, Characterization and Bio-Composites Application—A Review. *International Journal of Biological Macromolecules* **2016**, *93*, 789–804.
20. Kumar, S.; Negi, Y.S.; Upadhyaya, J.S. Studies on Characterization of Corn Cob Based Nanoparticles. *Adv. Mater. Lett* **2010**, *1*, 246–253.
21. Trache, D.; Hussin, M.H.; Haafiz, M.M.; Thakur, V.K. Recent Progress in Cellulose Nanocrystals: Sources and Production. *Nanoscale* **2017**, *9*, 1763–1786.
22. Yeasmin, S. Study of Acid Hydrolysis Based Synthesis of Microcrystalline and Nanocrystalline Cellulose from Local Lignocellulosic Materials. **2016**.
23. Hokkanen, S.; Bhatnagar, A.; Sillanpää, M. A Review on Modification Methods to Cellulose-Based Adsorbents to Improve Adsorption Capacity. *Water research* **2016**, *91*, 156–173.
24. Abu-Thabit, N.Y.; Judeh, A.A.; Hakeem, A.S.; Ul-Hamid, A.; Umar, Y.; Ahmad, A. Isolation and Characterization of Microcrystalline Cellulose from Date Seeds (Phoenix Dactylifera L.). *International journal of biological macromolecules* **2020**, *155*, 730–739.
25. Guo, J.; Guo, X.; Wang, S.; Yin, Y. Effects of Ultrasonic Treatment during Acid Hydrolysis on the Yield, Particle Size and Structure of Cellulose Nanocrystals. *Carbohydrate polymers* **2016**, *135*, 248–255.
26. Johar, N.; Ahmad, I.; Dufresne, A. Extraction, Preparation and Characterization of Cellulose Fibres and Nanocrystals from Rice Husk. *Industrial Crops and Products* **2012**, *37*, 93–99.
27. Trache, D.; Hussin, M.H.; Haafiz, M.M.; Thakur, V.K. Recent Progress in Cellulose Nanocrystals: Sources and Production. *Nanoscale* **2017**, *9*, 1763–1786.
28. Tarchoun, A.F.; Trache, D.; Klapötke, T.M.; Derradji, M.; Bessa, W. Ecofriendly Isolation and Characterization of Microcrystalline Cellulose from Giant Reed Using Various Acidic Media. *Cellulose* **2019**, *26*, 7635–7651, doi:10.1007/s10570-019-02672-x.

29. Adawiyah, R.; Suryanti, V. Preparation and Characterization of Microcrystalline Cellulose from Lembang (Typha Angustifolia L.). In Proceedings of the Journal of Physics: Conference Series; IOP Publishing, 2022; Vol. 2190, p. 012007.
30. Khili, F.; Borges, J.; Almeida, P.L.; Boukherroub, R.; Omrani, A.D. Extraction of Cellulose Nanocrystals with Structure I and II and Their Applications for Reduction of Graphene Oxide and Nanocomposite Elaboration. *Waste Biomass Valor* **2019**, *10*, 1913–1927, doi:10.1007/s12649-018-0202-4.
31. Guna, V.; Ilangovan, M.; K., A.; C.v., A.K.; C.v., S.; S., Y.; Nagananda, G.S.; Venkatesh, K.; Reddy, N. Biofibers and Biocomposites from Sabai Grass: A Unique Renewable Resource. *Carbohydrate Polymers* **2019**, *218*, 243–249, doi:10.1016/j.carbpol.2019.04.085.
32. Rouhou, M. C., Abdelmoumen, S., Thomas, S., Attia, H., & Ghorbel, D. Use of green chemistry methods in the extraction of dietary fibers from cactus rackets (Opuntia ficus indica): Structural and microstructural studies. International Journal of Biological Macromolecules, **2018**, 116, 901-910.
33. Cheng, D., Weng, B., Chen, Y., Zhai, S., Wang, C., Xu, R., & Guo, Y. Characterization of potential cellulose fiber from Luffa vine: A study on physicochemical and structural properties. International Journal of Biological Macromolecules, **2020**, 164, 2247-2257.
34. Chilukoti, G.R.; Mandapati, R.N. Characterization of Cellulosic Leaf Fiber from the Typha Angustifolia Plant. *Journal of Natural Fibers* **2022**, *19*, 2516–2526, doi:10.1080/15440478.2020.1819511.
35. Adeniyi, A.G.; Adeyanju, C.A.; Emenike, E.C.; Otoikhian, S.K.; Ogunniyi, S.; Iwuozor, K.O.; Raji, A.A. Thermal Energy Recovery and Valorisation of Delonix Regia Stem for Biochar Production. *Environmental Challenges* **2022**, *9*, 100630.
36. Abu-Thabit, N.Y.; Judeh, A.A.; Hakeem, A.S.; Ul-Hamid, A.; Umar, Y.; Ahmad, A. Isolation and Characterization of Microcrystalline Cellulose from Date Seeds (Phoenix Dactylifera L.). *International Journal of Biological Macromolecules* **2020**, *155*, 730–739, doi:10.1016/j.ijbiomac.2020.03.255.